Electronic Supplementary Material (ESI) for Energy & Environmental Science.

Self-Healing SEI Enables Full-Cell Cycling of Silicon-Majority Anode with Coulombic Efficiency Exceeding 99.9%

Yang Jin[acd†], Sa Li[b†], Akihiro Kushima[c†], Xiaoquan Zheng[a], Yongming Sun[d], Jin Xie[d], Jie Sun[d], Weijiang Xue[c], Guangmin Zhou[d], Jiang Wu[a], Feifei Shi[d], Rufan Zhang[d], Zhi Zhu[c], Kangpyo So[c], Yi Cui[de*], and Ju Li[cb*]

[a]State Key Lab of Electrical Insulation and Power Equipment, School of Electrical Engineering, Xi’an Jiaotong University, Xi’an 710049, P. R. China

[b] School of Materials Science and Engineering, Tongji University, 4800 Caoan Road, Shanghai 201804, China

[c]Department of Nuclear Science and Engineering and Department of Materials Science and Engineering, Massachusetts Institute of Technology, Cambridge, Massachusetts 02139, USA

[d]Department of Materials Science and Engineering, Stanford University, Stanford, California, 94305, USA

[e]Stanford Institute for Materials and Energy Sciences, SLAC National Accelerator Laboratory, 2575 Sand Hill Road, Menlo Park, California 94025, USA

[†]These authors contributed equally to this work.

[*]Corresponding authors: yicui@stanford.edu (Y.C.), liju@mit.edu (J.L.)

Supporting Figures

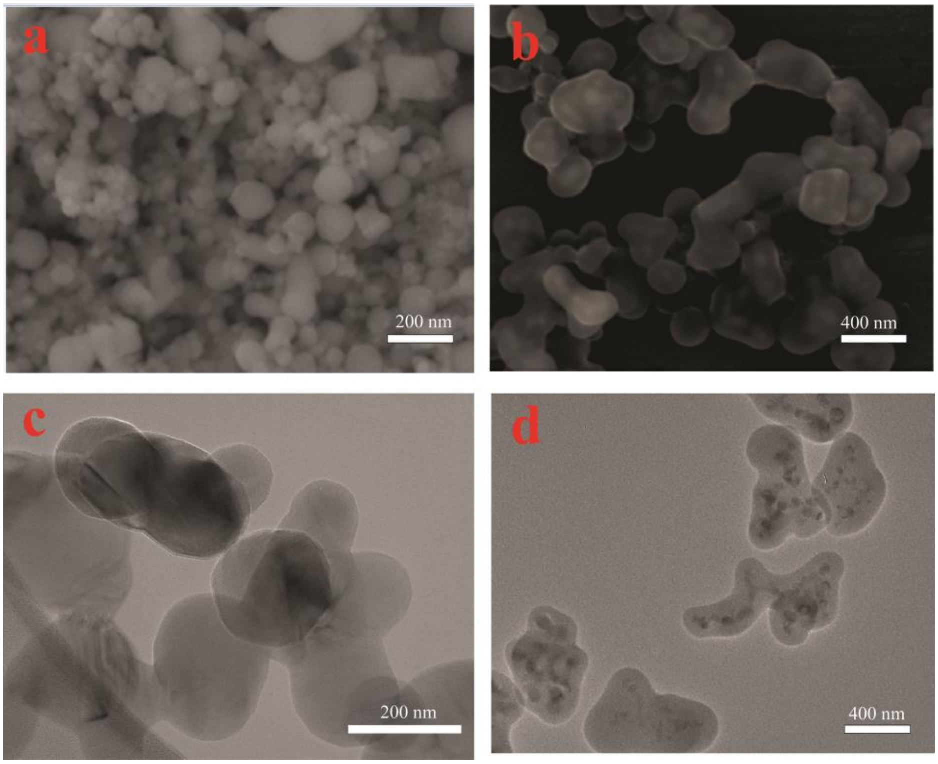

Supplementary Fig. S1. **Microstructures of Si@C nanocomposite after hydrothermal procedure**. **a**, SEM image of pure Si nanoparticles. Scale bar, 200nm. **b**, SEM image of the Si@C sample (7 g glucose, 70 mL DI water, 50mg Si nanoparticles, 170^{o}C for 8 h). Scale bar, 400 nm. **c**, TEM image of pure silicon nanoparticles. Scale bar, 200 nm. **d**, TEM image of the Si@C sample (7 g glucose, 70 mL DI water, 100 mg Si nanoparticles, 170 ^{o}C for 8 h). Scale bar, 400 nm.

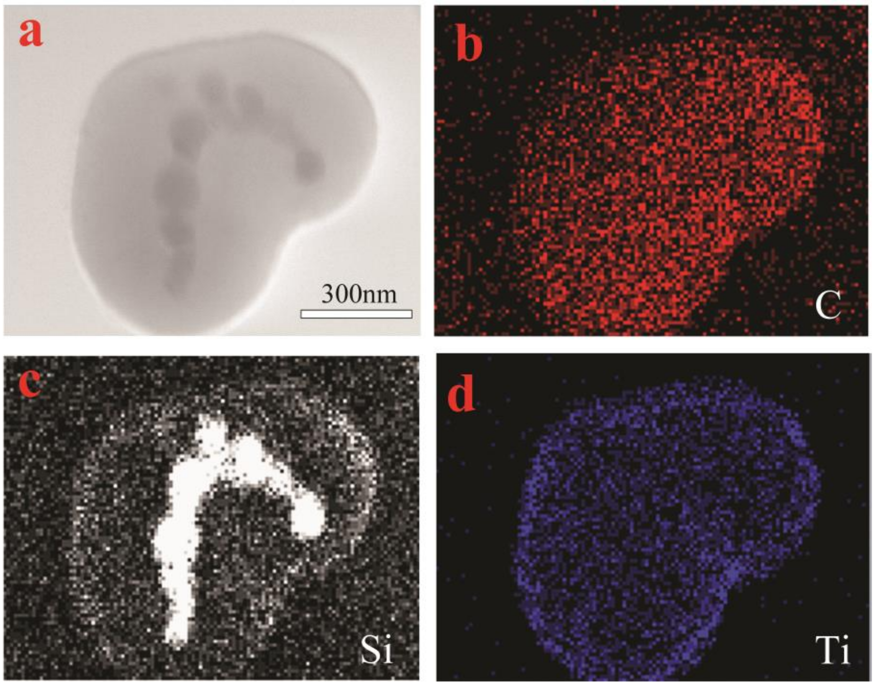

Supplementary Fig. S2. The STEM image (**a**) and chemical element mapping of C(**b**),Si(**c**) and Ti(**d**), after Titanium ion absorbing on the surface of Si@C, confirming the Si@C@$TiO(OH)_2$ structure. Scale bar, 300 nm.

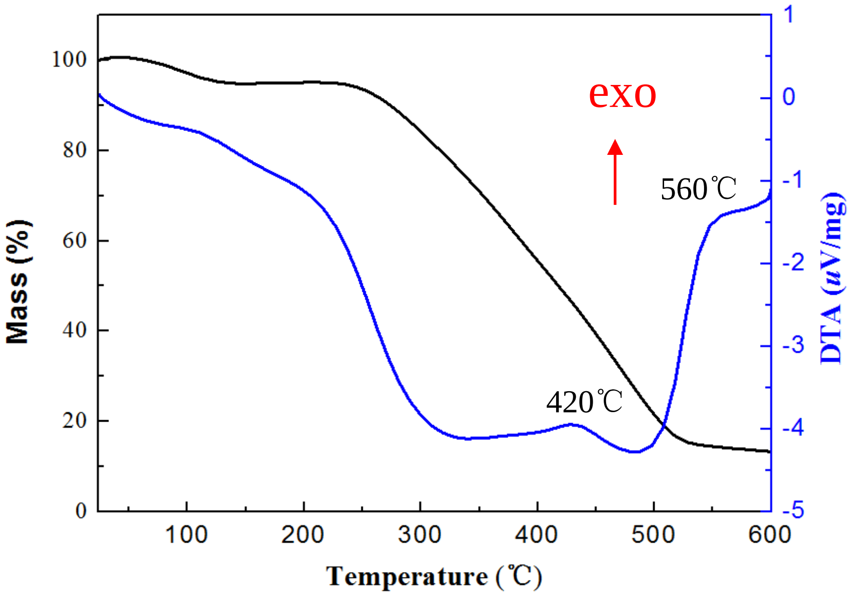

Supplementary Fig. S3. TG-DTA curve of the sample heated in simulated air atmosphere (20% O_2, 80% N_2, both are ultrapurity grade gases from Airgas) from room temperature to 600 °C at a heating rate of 10 °C /min.

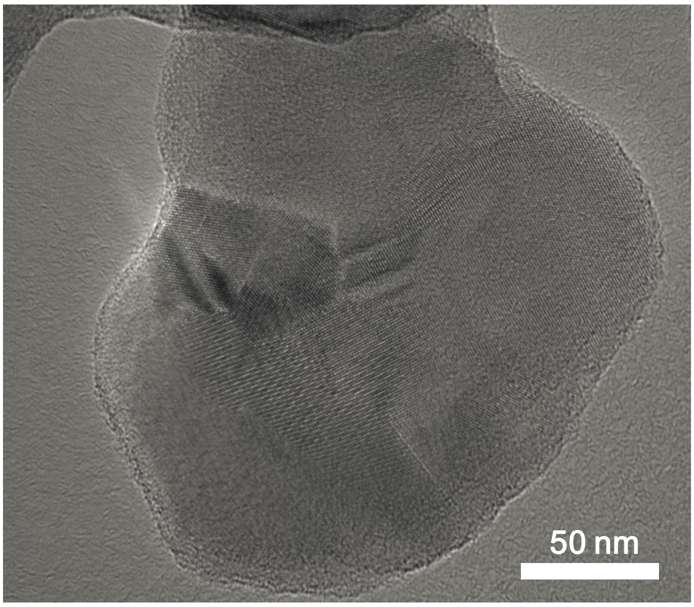

Supplementary Fig. S4. TEM image of pristine Si nano particle.

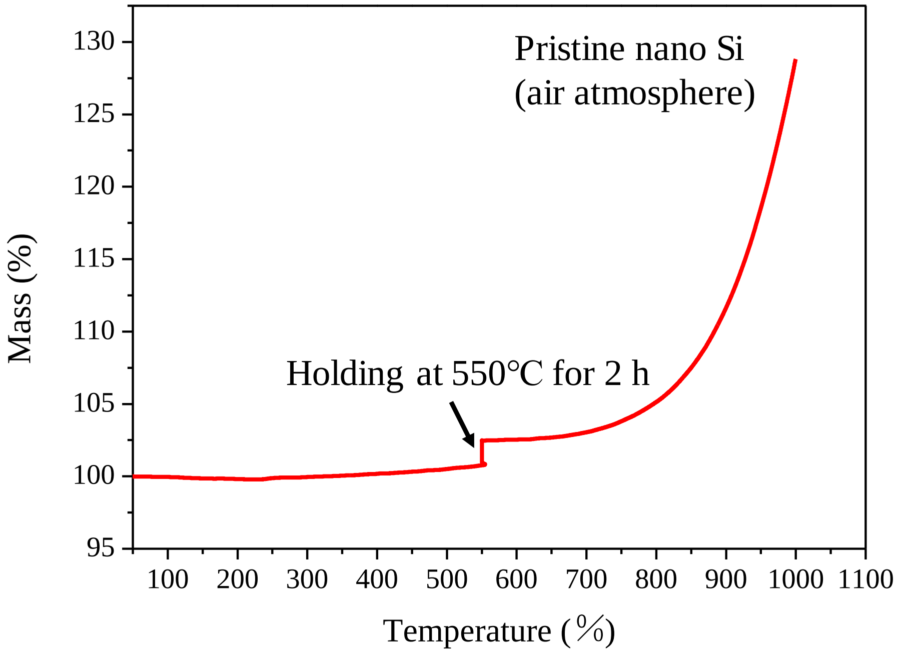

Supplementary Fig. S5. TG curve of commercial nano silicon powder heated in air atmosphere from room temperature to 1000 °C at a heating rate of 5 °C /min.

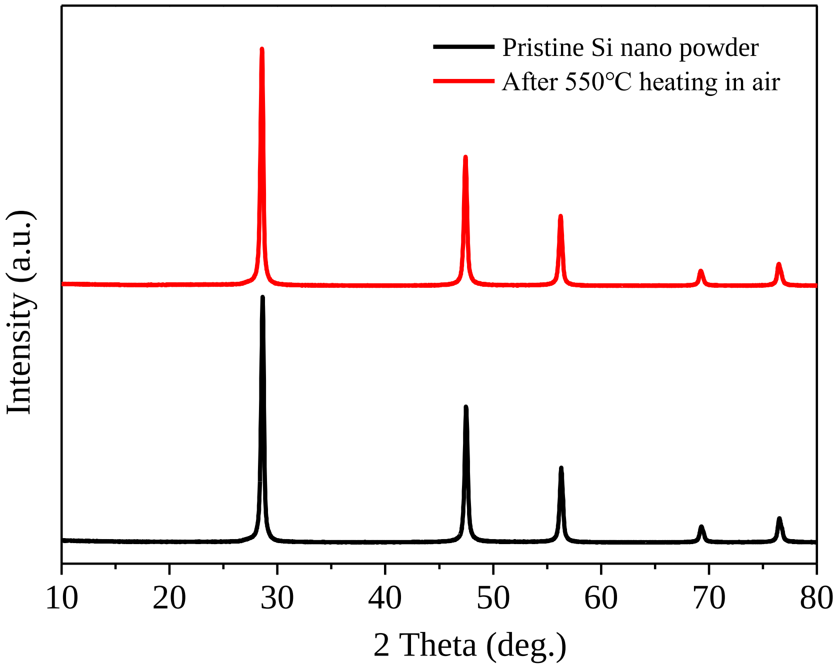

Supplementary Fig. S6. XRD data of commercial nano Si powder before and after 550 ℃ heat treatment in air atmosphere.

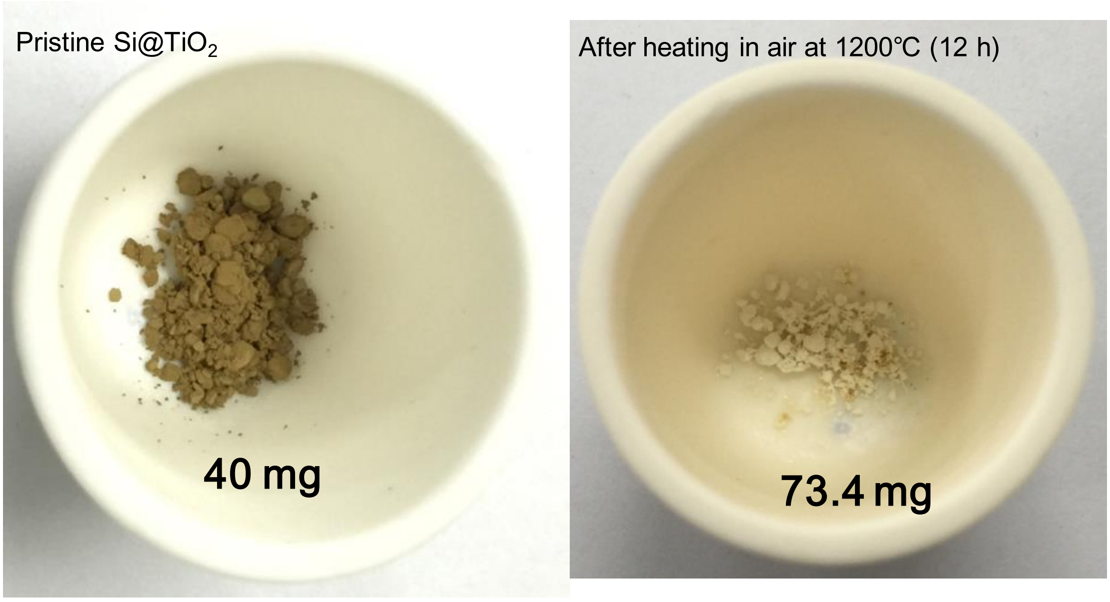

Supplementary Fig. S7. Weight data of Si@TiO_2 anode before and after 1200 ℃ heat treatment in air atmosphere for 12 h.

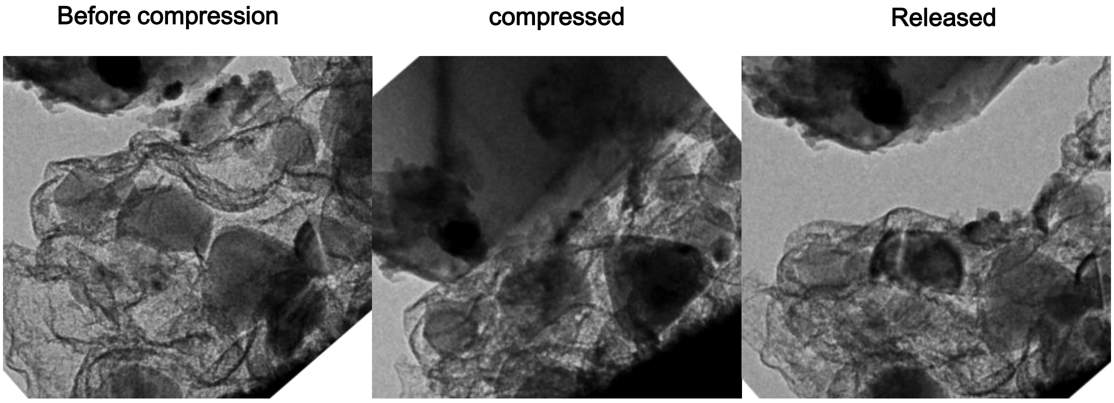

Supplementary Fig. S8. In-situ TEM press experiment of yolk-shell Si@TiO_2 cluster. Left, middle, and right images correspond to the initial, compressed, and load released states, respectively. To obtain the stress, the load was calculated by the displacement of the AFM cantilever tip and the contact area was estimated to be a circular shape with a radius of 150 nm for the compression, respectively. See also Supplementary movies S4.

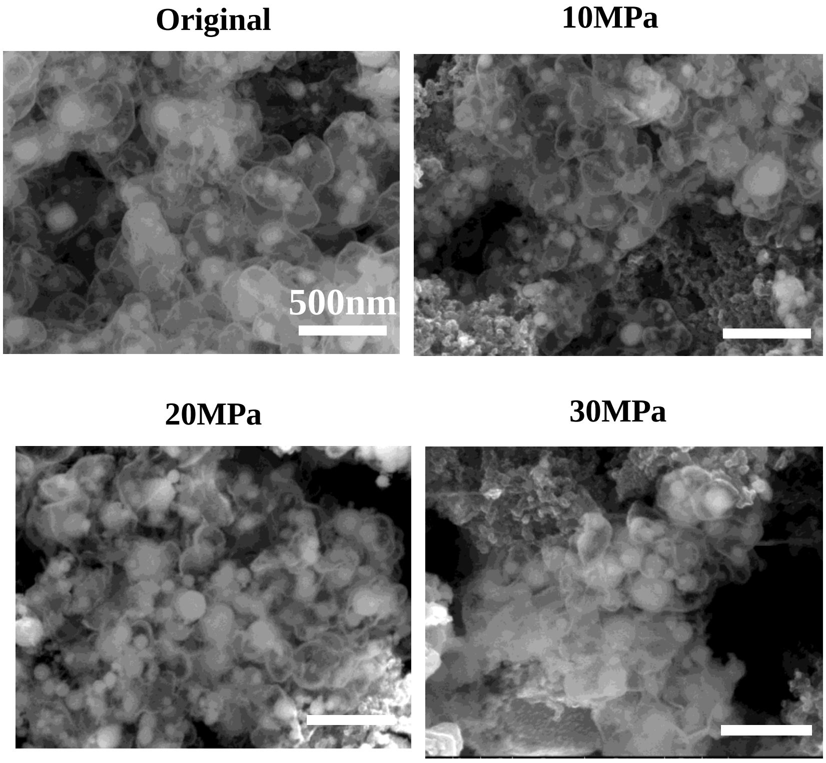

Supplementary Fig. S9. SEM images of yolk-shell Si@TiO_2 clusters electrode under different pressure.

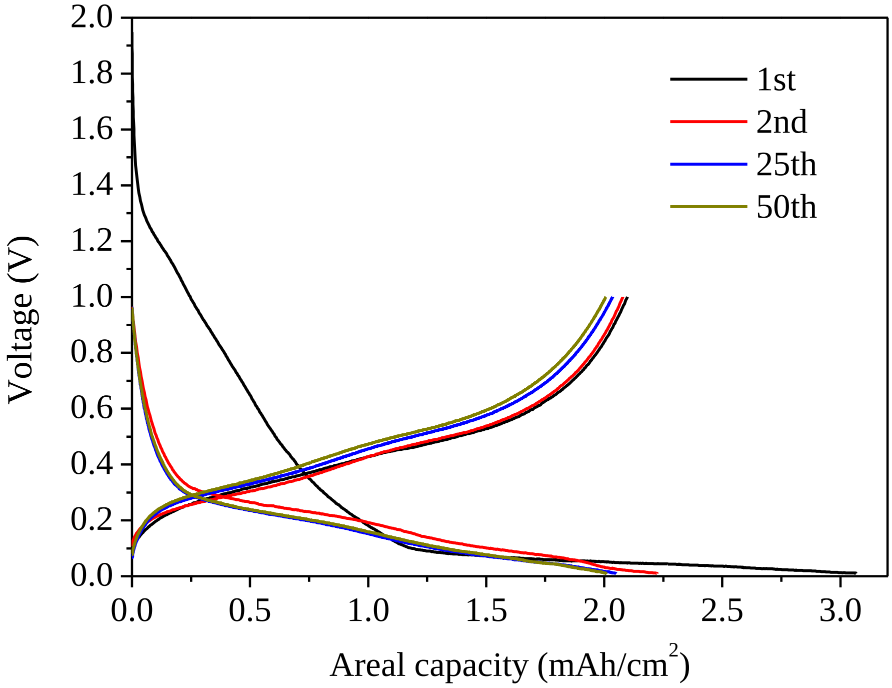

Supplementary Fig. S10. Si@TiO_2 cluster electrode (2.1 mg/cm^2) half cell charge/discharge voltage profiles with the 1st, 2nd and 25th and 50th cycling.

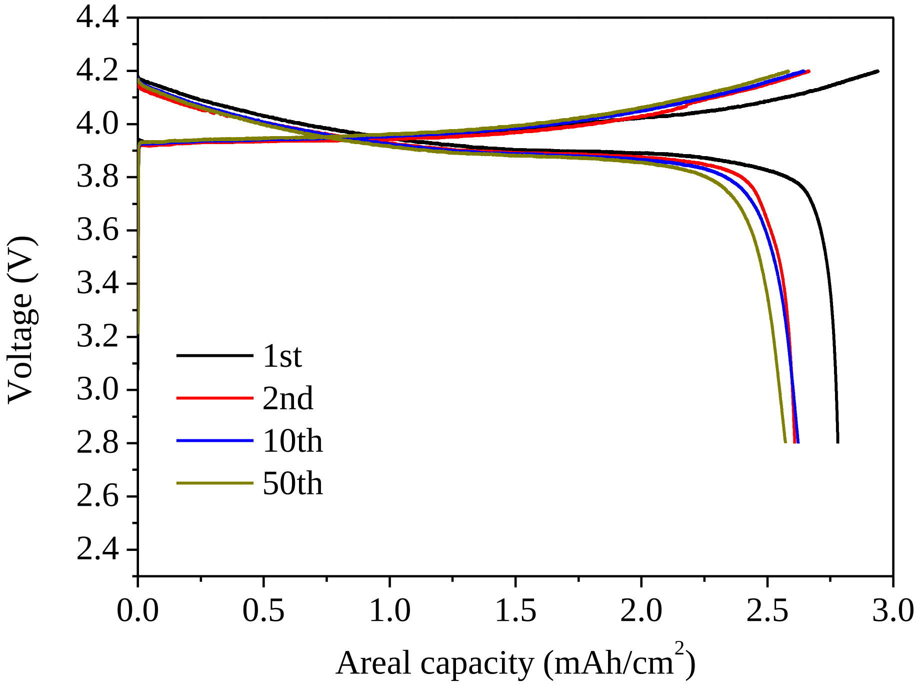

Supplementary Fig. S11. LCO half cell charge/discharge voltage profiles with the 1st, 2nd and 10th and 50th cycling.

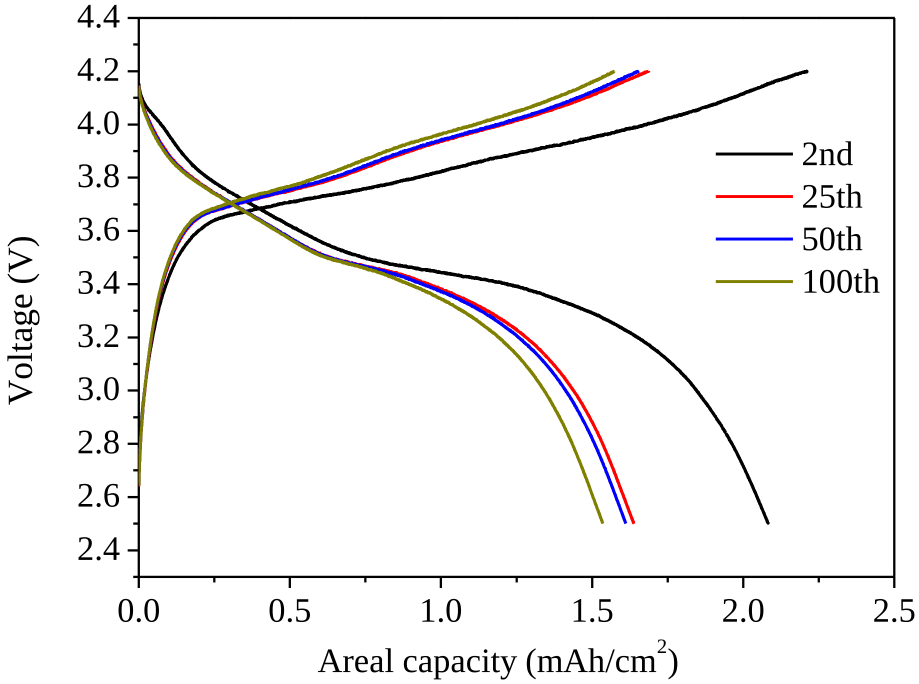

Supplementary Fig. S12. Si@TiO_2-LCO full cell charge/discharge voltage profiles with the 2nd, 25th and 50th and 100th cycling.

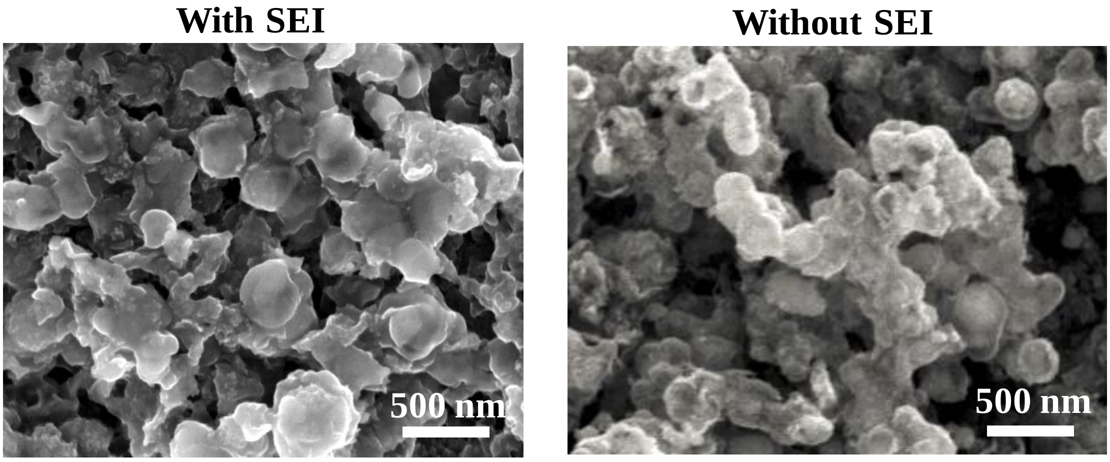

Supplementary Fig. S13. SEM images of Si@TiO_2 electrode with SEI and without SEI (using acid to remove surface SEI) after 100th cycling (delithiation stage).

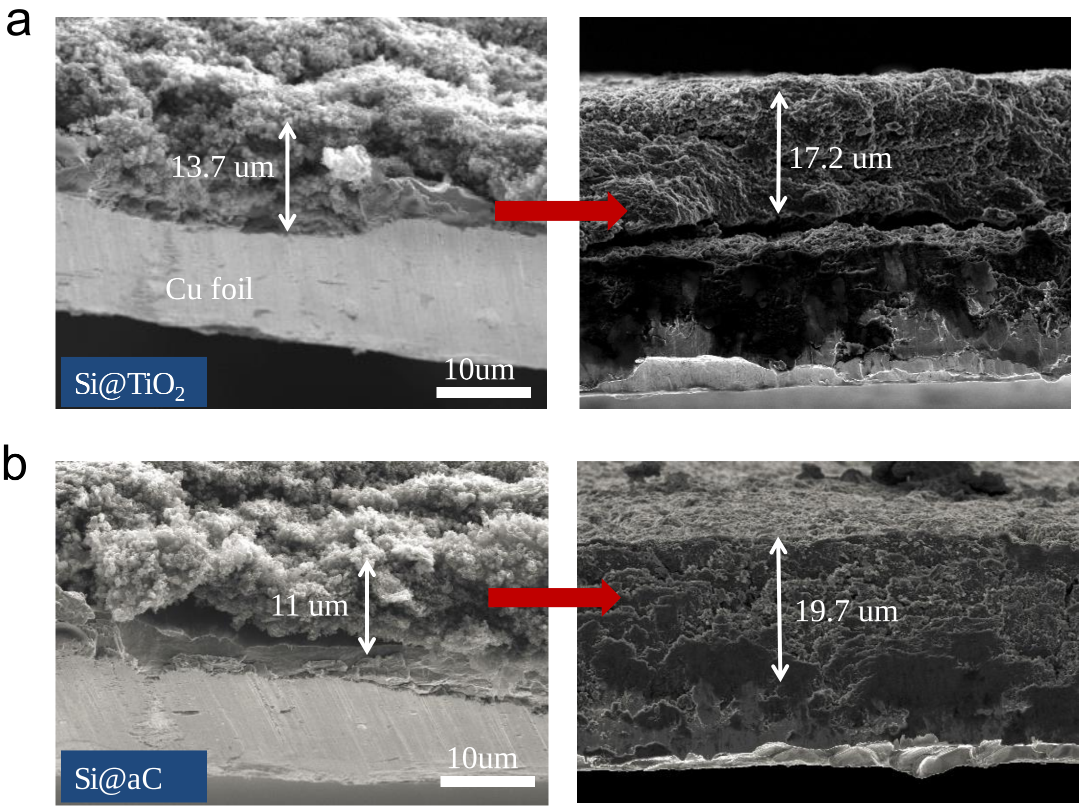

Supplementary Fig. S14. Si@TiO$_2$ (a) and Si@aC (b) electrode after 30MPa compression and after 100th cycling (delithiation stage).

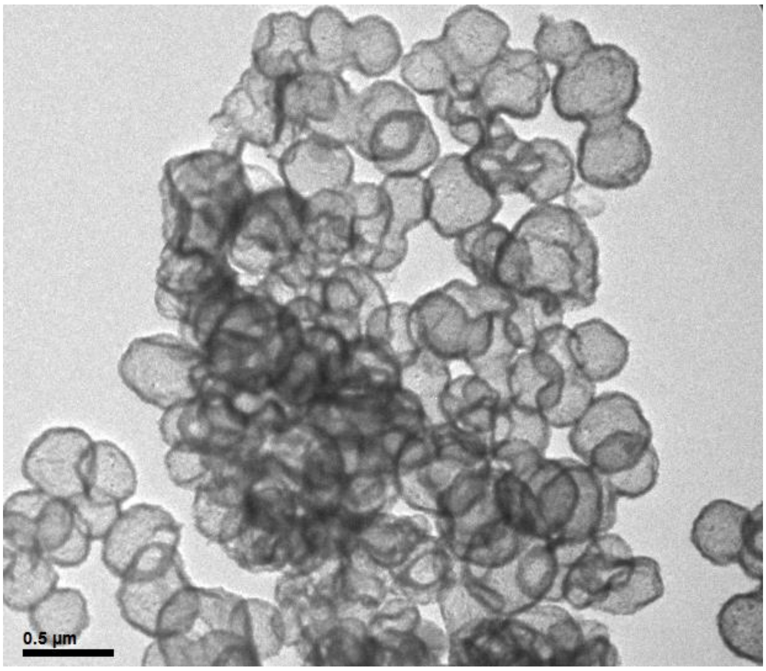

Supplementary Fig. S15. TEM image of pure hollow TiO$_2$ (without silicon) prepared using the NaOH etching the Si@C nanocomposite after hydrothermal. The following process stays the same. The obvious contrast between the edge and the center also reveals its hollow nature. Scale bar, 0.5 um.

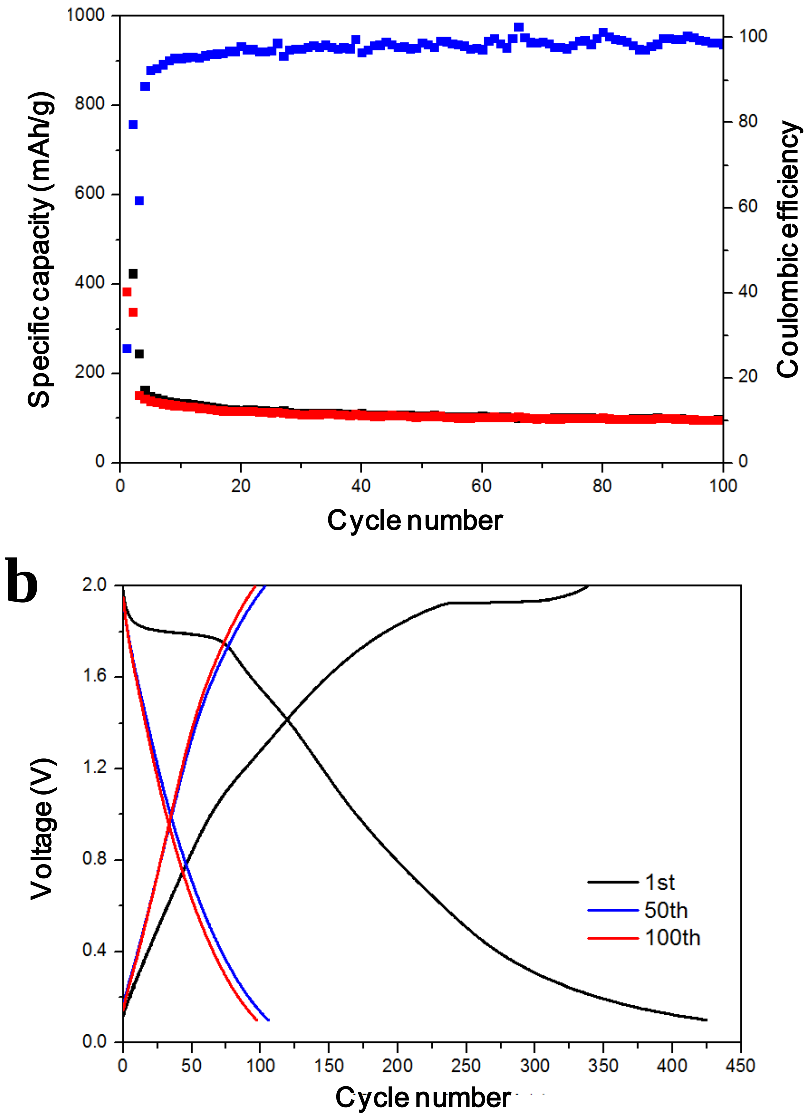

Supplementary Fig. S16. Electrochemical performance of hollow TiO_2. (a) Cycling life and the corresponding Coulombic efficiency in 100 cycles. (b) Charge/discharge voltage profiles with the 1st, 50th and 100th cycling.

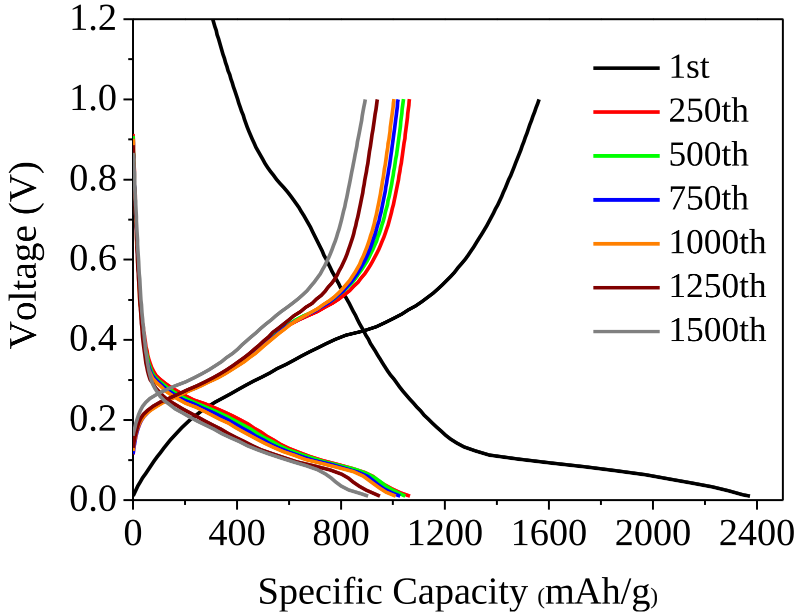

Supplementary Fig. S17. Si@TiO_2 half cell charge/discharge voltage profiles with the 1st, 250th and 500th, 750th and 1000th, 1250th and 1500th cycling.

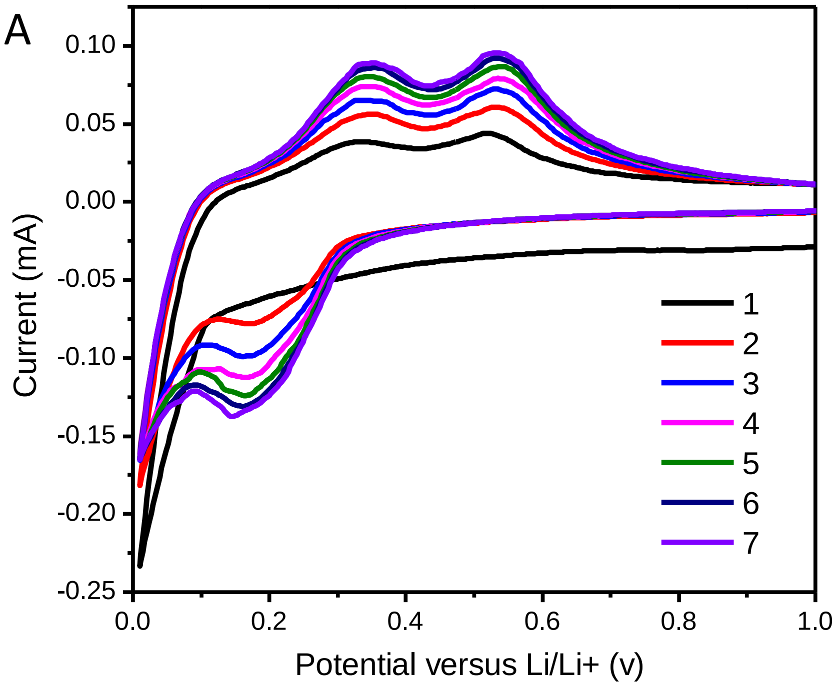

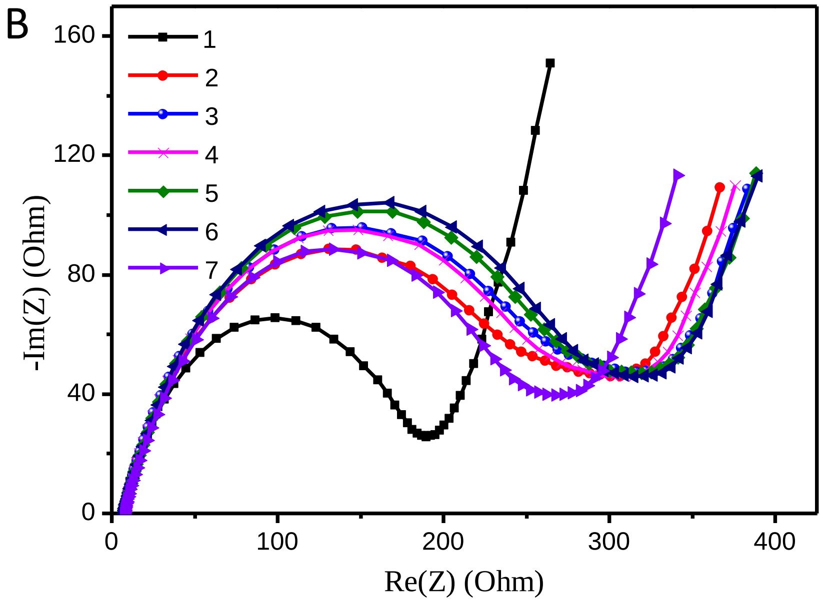

Supplementary Fig. S18. A. Cyclic voltammogram (CV) for Si@TiO_2 from 1.0 V to 0.01 V versus Li/Li^+ at a 0.05 mV/s scan rate. The first seven cycles are shown. **B.** EIS results for the same cell showing the evolution of the real and imaginary impedance after each cycle of CV scan. "1" in legend means before CV.

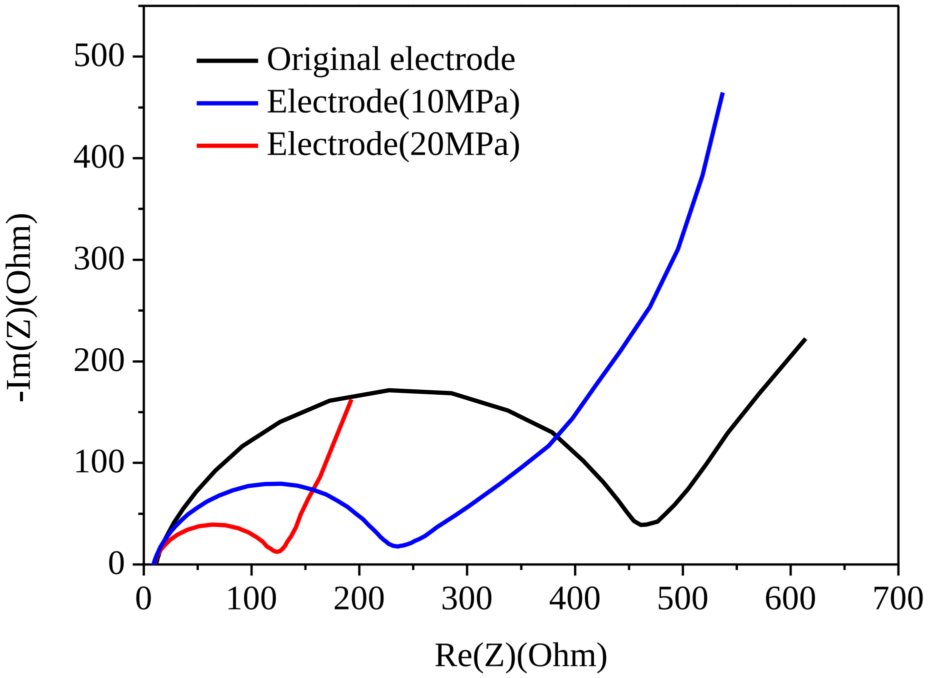

Supplementary Fig. S19. EIS results for the battery cell (Si@TiO_2 cluster electrode was under no pressure, 10 MPa and 20 MPa) showing the evolution of the real and imaginary impedance.

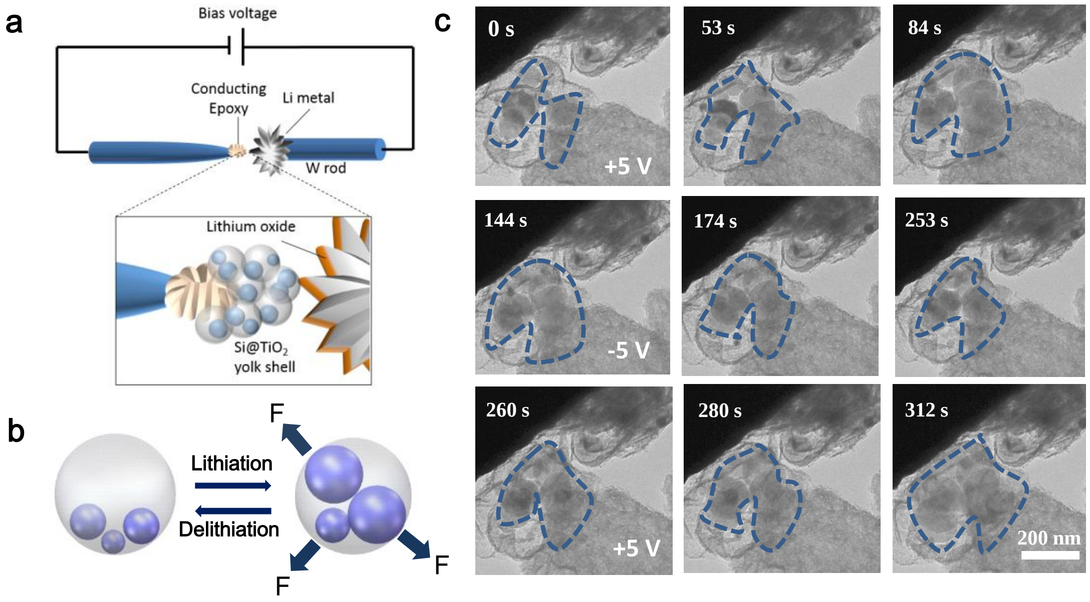

Supplementary Fig. S20. In situ TEM characterization during lithiation/delithiation. **a**. Schematic of the in situ TEM device. **b**. Schematic of silicon expansion and shrinkage in TiO_2 framework during lithiation/delthiation. **c**. Time-lapse images of the lithiation/delithiation of yolk-shell Si@TiO_2 cluster with insufficient void space (Supplementary Movie S3). Under a high voltage of 5 V, Lithium transports along and across the TiO_2 framework to react with the silicon inside, causing fast volume expansion. Although the void space is insufficient and the expanding silicon touch the TiO_2 shell, the framework still remains intact after two times lithiation(+5 V) and one time delithiation(-5 V).

Supplementary note 1: The effect of shell thickness on shell stiffness of TiO_2

Here, using a thin-walled sphere equation,

$$d = AFr(1-v^2)/Et^2,$$

where d is the displacement of the semispherical shell with thickness t, radius r, young's modulus E, and Poisson's ratio v, under force F, with A being a dimensionless constant (0.35), the stiffness F/d becomes,

$$Et^2/Ar(1-v^2).$$

So the stiffness of the sphere is proportional to the square of the wall thickness and the inverse of the radius.

The TiO_2 shells of our $Si@TiO_2$ have complex structure (in some cases interconnected) and are not perfect spheres. However, we can roughly estimate the stiffness using the above relationship. If we take the Young's modulus of TiO_2 to be 250 GPa, r =115 nm and t = 16 nm would give F/d = 1800 N/m. The actual measurement gives ~1000 N/m from Fig. 3e. So the agreement is decent. The discrepancy should arise from the fact that (a) the Young's modulus of nanoshell has size effect, well known from measurement of nanowires[1], and (b) the shell is not perfectly smooth (has roughness), so the projected shell thickness appears to be somewhat larger.

1. X.G. Wang, K. Chen, Y.Q. Zhang, J.C. Wan, O. L. Warren, J. Oh, J. Li, E. Ma, and Z.W. Shan. *Nano Lett.,* 2015, **15**, 7886-7892.

Supplementary note 2: The void volume calculation

The mass loading of Si@TiO_2 is 2.1 mg/cm^2 and the electrode thickness before pressing is 50 um. So the tap density of Si@TiO_2 electrode is calculated to be 0.42 g/cm^3. The density of Si is 2.3 g/cm^3 and the density of anatase is 3.8 g/cm^3. Based on the weight ratio of 7.3:2.7 (Si:TiO_2), the void volume can be calculated according to the following equation:

$$\begin{cases} 3.8V_{anatase} + 2.3V_{Si} = 1 \\ \dfrac{3.8V_{anatase}}{2.3V_{Si}} = \dfrac{0.27}{0.73} \\ \dfrac{1}{V_{Si} + V_{anatase} + V_{void}} = 0.42 \end{cases}$$

Where, V_{anatase} stands for the volume of anatase; V_{Si} stands for the volume of Si; V_{void} stands for the volume of void space before pressing.

And, the result was shown as following:

$$\begin{cases} V_{anatase} = 0.071 \\ V_{Si} = 0.317 \\ V_{void} = 1.99 \end{cases}$$

So before pressing, the void volume is about 6.3 times of the Si volume. The radius of shell is about 1.94 times of the radius of Si (R_{shell}=1.94R_{Si}).

After pressing (30 Mpa), the electrode was compressed to 14.7 um, so the compressed electrode density is 1.43 g/cm^3.

Then, the void volume can be calculated using the same method, as following:

$$\begin{cases} V_{anatase} = 0.071 \\ V_{Si} = 0.317 \\ V_{void} = 0.311 \ (after \ pressing) \end{cases}$$

So after pressing, the void volume was about the same as the Si volume. The electrode thickness stabilized at about 17.2 um after 20 cycles, when the TiO_2 framework already accommodate with the Si. The stabilized compressed density is 1.22 g/cm^3. Then, the stabilized void volume can be calculated as following:

$$\begin{cases} V_{anatase} = 0.071 \\ V_{Si} = 0.317 \\ V_{void} = 0.432 \ \ (stablized) \end{cases}$$

The stabilized area capacity is about 1.7 mAh/cm^2, and the mass loading of Si is about 1.533 mg/cm^2 (considering weight ratio Si:TiO_2=7.3:2.7). So the measured specific capacity of Si is about 1109 mAh/g, which means the electrochemical active Si ratio is about 26.4% (Si theoretical specific capacity 4200 mAh/g). The electrochemical active Si volume $V_{\text{active Si}}$ =0.317*0.264=0.08. So the stabilized void volume V_{void}=5.4 $V_{\text{active Si}}$. It is obvious that the void space is enough for the electrochemical Si expansion.

Supporting Movies

Supplementary Movie S1. In situ pressing experiment of hollow carbon sphere. The movie is played at 10x speed.

Supplementary Movie S2. In situ pressing experiment of hollow TiO_2 sphere. The movie is played at 10x speed.

Supplementary Movie S3. In situ pressing experiment of Si@TiO_2 cluster. The movie is played at 10x speed.

Supplementary Movie S4. In situ pressing experiment of Si@TiO_2 cluster. The movie is played at 10x speed.

Supplementary Movie S5. Lithiation of a Si@TiO_2 yolk-shell cluster. The SiNPs expand towards the void spaces and the TiO_2 shell is stable upon lithiation. The movie is played at 25x speed.